

## RESEARCH ARTICLE

# Responses to mechanically and visually cued water waves in the nervous system of the medicinal leech

Andrew M. Lehmkuhl<sup>1</sup>, Arunkumar Muthusamy<sup>1</sup> and Daniel A. Wagenaar<sup>1,2,\*</sup>

## ABSTRACT

Sensitivity to water waves is a key modality by which aquatic predators can detect and localize their prey. For one such predator – the medicinal leech, *Hirudo verbana* – behavioral responses to visual and mechanical cues from water waves are well documented. Here, we quantitatively characterized the response patterns of a multisensory interneuron, the S cell, to mechanically and visually cued water waves. As a function of frequency, the response profile of the S cell replicated key features of the behavioral prey localization profile in both visual and mechanical modalities. In terms of overall firing rate, the S cell response was not direction selective, and although the direction of spike propagation within the S cell system did follow the direction of wave propagation under certain circumstances, it is unlikely that downstream neuronal targets can use this information. Accordingly, we propose a role for the S cell in the detection of waves but not in the localization of their source. We demonstrated that neither the head brain nor the tail brain are required for the S cell to respond to visually cued water waves.

**KEY WORDS:** *Hirudo verbana*, Electrophysiology, S cell, Sensory systems, Aquatic predators

## INTRODUCTION

Aquatic predators utilize a wide variety of sensory modalities to localize their prey. Some use modalities that are also available to predators in other environments, such as the larvae of the gray treefrog, *Hyla versicolor*, which use chemosensation (Troyer and Turner, 2015), and toothed whales, which use echolocation (Wilson et al., 2007). Others rely on modalities that are only available under water, such as electric eels, which use electroreception (Hagiwara et al., 1965). Yet others rely on the detection of physical disturbances to the water created by their prey. Such indirect detection of prey is widely spread through the animal kingdom and has been described in arrow worms (Horridge and Boulton, 1967), insects (Lang, 1980), spiders (Bleckmann and Barth, 1984), toads (Elepfandt, 1984), dogfish (Russell and Roberts, 1974), and seals (Dehnhardt et al., 1998; Zimmer, 2001). The medicinal leech, *Hirudo verbana*, is also in this category as it utilizes water surface waves to guide predation (Young et al., 1981). Serological studies on bloodmeals (Wilkin and Scofield, 1990) have shown that its diet is composed of blood from frogs, fishes, birds and mammals.

Water waves provide multiple forms of sensory information that can be used to interpret the nature of those waves and – more importantly – the agent responsible for causing them. When a prey animal moves through the water, pressure waves emanate from its location and provide directional cues to predators. Prey animals may also generate surface waves that propagate centrifugally and cause detectable water movement at a distance. In addition to bulk water movement, propagating surface waves also cause the refraction of sunlight by the water surface to fluctuate. The resulting alternation of light and shadow cast into the water yields visual cues that can be used as a directional cue.

Medicinal leeches can sense water motion using mechanosensory hairs distributed in a grid along their bodies. These ‘sensillar movement receptors’ (SMRs) provide directional information about the source of surface waves (Young et al., 1981). Additionally, leeches can use visual information (Dickinson and Lent, 1984; Carlton and McVean, 1993) through an array of visual sensilla co-localized with the mechanosensory hairs and several pairs of simple eyes located in the head (Röhlich and Török, 1964; Kretz et al., 1976). The visual sensilla, of which there are seven pairs in each of the animal’s 21 mid-body segments, appear especially well positioned to detect the direction of passing light and shadows. Leeches do not have image-forming eyes that could be used to see prey directly.

When both mechanical and visual cues are available for prey localization, adult leeches rely preferentially on mechanical cues (Harley et al., 2011), but in the absence of mechanical cues, they can still localize their prey using visual cues alone. This implies that leeches must possess neuronal circuits that allow them to discriminate between different visual or mechanical cues and to assess the direction of the surface waves that give rise to those cues. However, although several neurons have been identified as downstream targets of the sensillar photoreceptors (Kretz et al., 1976), these circuits remain unknown.

Predation evidently involves integration of sensory information across modalities as well as across segments so that the animal can ultimately reach a unitary decision to guide locomotion. Only one cell is known in the leech that responds to both visual and mechanical inputs (Bagnoli et al., 1973). This cell is known as the S cell, and occurs as a single unpaired neuron in each of the leech’s 21 segmental ganglia (Laverack, 1969). The S cell not only integrates information across sensory modalities, it is also uniquely positioned to integrate information across segments: each S cell sends axons into the anterior and posterior medial connectives (‘Faivre’s nerve’), where they form electrical synapses with the S cells of neighboring segmental ganglia (Frank et al., 1975). [The nervous system of the leech consists of 21 segmental ganglia, four cephalic ganglia that are fused to form a ‘head brain’, and seven caudal ganglia that are fused to form a ‘tail brain’ (e.g. Wagenaar, 2015).] The coupling between adjacent S cells is so strong that all the S cells together form a single electrical syncytium in which

<sup>1</sup>University of Cincinnati, Department of Biological Sciences, Cincinnati, OH 45221, USA. <sup>2</sup>California Institute of Technology, Division of Biology and Biological Engineering, Pasadena, CA 91125, USA.

\*Author for correspondence (daw@caltech.edu)

© A.M.L., 0000-0002-5712-2012; A.M., 0000-0002-1804-586X; D.A.W., 0000-0002-6222-761X

action potentials readily propagate along the full length of the animal.

According to Bagnoli et al. (1973), the S cell responds to acute mechanical stimuli (brief touches with a mechanically driven poker) with short bursts of action potentials. They further reported that the S cell responds in a similar manner to flashes of light, but not to sustained mechanical stimuli. Responses to mechanical stimuli were found to occur at a shorter latency than those to visual stimuli and briefly caused the cell to become refractory to visual stimuli. In contrast, when the latency between a mechanical pulse and a subsequent visual flash was increased, the visual response was enhanced.

These results clearly established the S cell as part of a pathway of cross-modal sensory integration. Little is known, however, of the role of the S cell in more complex, more behaviorally relevant stimulus responses. In particular, it is not known whether and how the S cell responds to the periodic low-intensity mechanical or visual sensory inputs provided to the animal by water waves. Given the role of the S cell in both sensory integration and interganglionic spatial integration, we hypothesized that it would be well positioned to respond to and interpret complex wave stimuli. Therefore, we decided to choose the S cell as a starting point for investigating the neuronal basis of prey detection.

## MATERIALS AND METHODS

### Animal care

Adult medicinal leeches (*Hirudo verbana* Cerna 1820) were obtained from Niagara Medicinal Leeches (Westbury, NY, USA) and maintained according to methods described by Harley et al. (2011). Briefly, leeches were maintained in tanks of 20–40 individuals in a temperature-controlled room held at 15–16°C with a 12h:12 h light:dark cycle. All leeches used in this study had fasted for 2–4 months and weighed 1.1–2.7 g at the time of the experiments.

### Electrophysiology

Leeches were anesthetized in ice-cold saline (Muller et al., 1981) and immobilized on slabs of transparent polydimethylsiloxane (PDMS; Sylgard 184, Dow Corning) to allow access to the segmental ganglia. For experiments involving visual cues, leeches were pinned dorsal side down, to allow visualization and electrode access from above and visual stimulation from below. The body wall was opened up along the ventral mid-line to expose the nerve cord between segments 8 and 12. For experiments involving mechanical cues, leeches were pinned dorsal side up and the body wall was opened up along the dorsal mid-line. For both visual and mechanical experiments, the lateral roots of ganglia 9 to 11 were cut and those three ganglia were immobilized using fine tungsten pins on a thin, rectangular slab of PDMS. In the context of leech electrophysiology, these preparations can be considered ‘nearly intact’, as similarly prepared leeches are known to exhibit approximately normal swimming behavior (Kristan et al., 1974) and much more reduced preparations still exhibit essential features of reproductive behaviors (Wagenaar et al., 2010). Critically, in the mechanical experiments, the cilia on the dorsal side remain in contact with the water as normal, and in the visual experiments, the light path to the sensilla is essentially unobstructed.

Action potentials in the S cell were recorded extracellularly using two en passant suction electrodes applied to the ventral nerve cord on either side of ganglion 10. (In some of the experiments presented in Fig. 4A, we recorded anteriorly and posteriorly to a different ganglion, in which case the lateral roots of that ganglion and its

immediate neighbors were cut rather than those of ganglia 9–11.) Signals were amplified using a differential AC amplifier (A-M Systems model 1700) and visualized using VScope (Wagenaar, 2017).

In extracellular recordings from the ventral nerve cord, the largest spikes consistently correspond to action potentials in the S cell (Frank et al., 1975). As action potentials travel along axons at a finite speed, timing differences between spikes detected at an anterior location and at a posterior location can be used to infer the direction of propagation of the action potential. In our experiments, the largest unit in the anterior electrode always fired in close temporal proximity to the largest unit in the posterior electrode, with a latency of several milliseconds in either direction (Fig. 3C). The precise latency varied between preparations (as a consequence of variability in precise placement of electrodes), but in all cases, histograms of observed latencies (Fig. 3C, right) exhibited two clearly distinct peaks corresponding to rostrocaudal and caudo-rostral propagation, respectively. In a few recordings, a third much smaller peak occurred around zero latency. As we could not unequivocally determine whether those events corresponded to action potentials originating in the ganglion between the electrodes or to synchronized noise pick-up, such events were discarded.

### Mechanical wave generation

A function generator (Pasco Scientific, Roseville, CA, USA) powered two loudspeakers to move a hollow aluminium bar up and down to produce approximately sinusoidal waves in a glass aquarium filled to a depth of 2.4 cm with cold saline. Wave amplitude and frequency were controlled via the function generator. Leeches, immobilized on a PDMS platform and prepared as described above, were placed at a distance of 18 cm from the wave source, in a location where waves propagated approximately linearly. To reduce the influence of visual cues, all experiments were performed in the dark while the room light was turned on between trials to prevent dark adaptation of the animal’s visual system.

To be able to mimic the characteristics of the physical waves in the visual modality (see below), we determined the dispersion relation of the physical waves, i.e. measured their wavelength as a function of frequency. To do so, we placed an array of shiny vertical metal posts immediately behind the aquarium and illuminated those with bright red light in an otherwise dark room. This resulted in very distinct reflections that undulated in the generated waves (Fig. S1A). The relative phases of the undulations of the reflections of all of the posts were reconstructed based on video recordings of waves of various frequencies (Fig. S1C). (This was straightforward because the reflections of the posts were so bright that their locations could be extracted by simple thresholding of the image sequence; Fig. S1B.)

We verified that waves propagated linearly and calculated wavelengths ( $\lambda$ ) by fitting the phases  $\phi(x)$  at each location  $x$  to  $\phi(x)=2\pi x/\lambda$ . This procedure was repeated at many different frequencies, not just those ultimately used in our experiments, to obtain the most accurate results. We had expected that the relation between wavelength and frequency ( $f$ ) would fit the textbook equation for gravity waves (e.g. Rizzoli, 2008):  $f=\sqrt{[(g/2\pi\lambda)\tanh(2\pi h/\lambda)]}$ , where  $h$  is the depth of the water (2.4 cm) and  $g$  is the gravity acceleration (9.81 m s<sup>-2</sup>). However, the fit turned out to be poor, so we derived an empirical dispersion relation instead. We found that a power law relation:  $1/\lambda=Af^B$  fitted the data well (Fig. S1D). Best-fit parameters were  $A=0.020$  and  $B=1.41$  when frequencies were measured in hertz and wavelengths in centimeters.

**Table 1. Dispersion relation for visually cued virtual waves, empirically based on measurements of physical waves**

Frequency (Hz)	0.5	1	2	4	8	16
Wavelength (cm)	135	50.5	19.0	7.12	2.67	1.00

The results of this exercise, as used in the subsequent visual experiments, are given in Table 1.

### Determination of wave amplitude

To accurately determine wave amplitude for the mechanical experiments, we proceeded as follows. A laser beam was aimed perpendicularly to the wave fronts at a downward angle of 45 deg. Sawdust was sprinkled onto the surface of the water to illuminate the point where the laser hit the water surface. (We presumed that the weight of sawdust impacted the characteristics of the waves being produced marginally at most, and thus did not influence measurements, but we did not quantitatively verify this assumption.)

Videos of waves were then recorded from an approximately horizontal angle to the water surface. In these videos, brightly lit sawdust particles effectively represented the surface of the water under the laser spot, moving vertically and horizontally with incoming waves. Using custom software (written in Octave) to track bright spots in each video, the movement of the water was measured in the direction of wave propagation and in the vertical direction. For each relevant frequency, we measured the wave amplitude at various driving voltages of the function generator to obtain a calibration curve. These curves then allowed us to produce waves of precisely determined amplitudes at all frequencies. At frequencies below 1 Hz, we found that significant bulk water displacement accompanied the surface waves, complicating interpretation of biological responses. Accordingly, we did not include mechanical wave experiments at frequencies below 1 Hz in this paper.

As it was not possible to image with the camera perfectly horizontal due to the meniscus of the water against the aquarium wall, water movement perpendicular to the direction of wave propagation (towards or away from the camera) could potentially affect the motion estimate in the vertical direction. To quantify this effect, additional videos were recorded with the camera mounted above the aquarium and facing downward onto the water surface. From these videos we determined that perpendicular water movements were so small that their effect on vertical measurements was at most 4  $\mu\text{m}$ , and were hence negligible.

### Visual wave and flash generation

Previous experiments had shown that leeches responded to visually cued virtual waves generated using a video projector in a manner indistinguishable from their responses to actual water waves that they could sense visually but from which they were mechanically isolated (Harley et al., 2011). As projecting visual waves is much more straightforward and allows tighter experimental control than using actual waves, we exclusively used projected waves for the visual experiments in this study.

Specifically, visual waves were projected from below onto the dorsal surface of a leech using the green channel of a Pico Projector (AAXA Technologies Inc., Irvine, CA, USA) and a mirror. All visual waves were nominally sinusoidal and were generated in accordance with the empirical dispersion relation of Table 1. (Please note that ‘wavelength’ in Table 1 refers to the period of the visual pattern, not to the wavelength of the light.) Illuminance was measured at the location of the leech using an LX1330B digital illuminance/light meter (Dr Meter). The peak intensity of the

projected waves was 208 lux of green light; the trough intensity was 10 lux. (All our lux measurements are accurate to 10% in absolute value due to the limited accuracy of the meter. Inter-trial and inter-animal variations were below the measurement accuracy.) The background illumination of the rest of the room was around 1 lux. In the ablation experiments (Fig. 4), full body flashes of 0.34, 3.4, 34 and 340 lux were used while the room was illuminated with 3.3 lux. These flash intensities were derived from the full strength of the projector using absorptive neutral density filters (Thorlabs, Newton, NJ, USA).

### Data analysis

Most results in this paper are expressed in terms of simple absolute spike counts over a particular interval during stimulation. These counts are always of verified S cell spikes based on detecting the spike on both electrodes with an appropriate inter-electrode latency, as outlined above. The intervals used for analysis were based on standout features of typical responses: as wave stimuli typically resulted in a strong initial response followed by a weaker sustained response that qualitatively varied for different wave frequencies (Fig. 1), we analysed the initial phase and the sustained phase of the response separately. We defined the end of the initial phase to be 1 s after the median latency of the first spike in a given stimulus condition; the sustained phase ended 10 s later. (The results did not change significantly if we varied these criteria by several hundred milliseconds.)

For the ablation experiments reported in Fig. 4, stimuli were trains of three flashes with 50% duty cycle presented at 1.5 Hz (i.e. 0.33 s light on, 0.33 s light off, total train duration 1.67 s). In these experiments, we did not distinguish between an early and a late phase of responses, and instead counted spikes over a 2.5 s interval starting from the onset of the stimulus. (The counting interval extended 500 ms past the end of the stimulus train to allow for response delays.)

For technical reasons, the experiments on frequency dependence in the mechanical modality (Fig. 2A,B) were performed at different but broadly overlapping sets of wave amplitudes for the various frequencies. (The reason was that establishing an accurate and reliable relationship between the driving voltage of the speaker and the resulting wave amplitude proved much more challenging than we initially expected; see above. The time constraints of the project forced us to perform the mechanical stimulation experiments before this relationship was fully determined.) Before graphing the data, the resulting raw counts were therefore interpolated to a common set of wave amplitudes (50, 100, 150 and 200  $\mu\text{m}$ ) for each frequency. All amplitudes were measured peak-to-peak and in no case were data extrapolated beyond the measurement range.

## RESULTS

Wave stimuli readily evoked spikes in the S cell. This was true for both mechanical waves presented in darkness (Fig. 1A) and for visually cued virtual waves (hereafter referred to as ‘visual waves’; Fig. 1B). Both modalities elicited a strong initial response followed by a weaker sustained response that was most prominent for low-frequency visual waves (Fig. 1C,D). Cessation of mechanical stimulation but not of visual stimulation occasionally elicited a weak off-response (Fig. 1C). This may have been due to a slight mechanical jerk as the speaker stopped moving.

Previously, it had been shown that leeches most readily localize mechanically cued wave sources at frequencies around 8–12 Hz, whereas they most readily localize visually cued wave sources at frequencies around 2 Hz (Harley et al., 2011). To test whether S cell

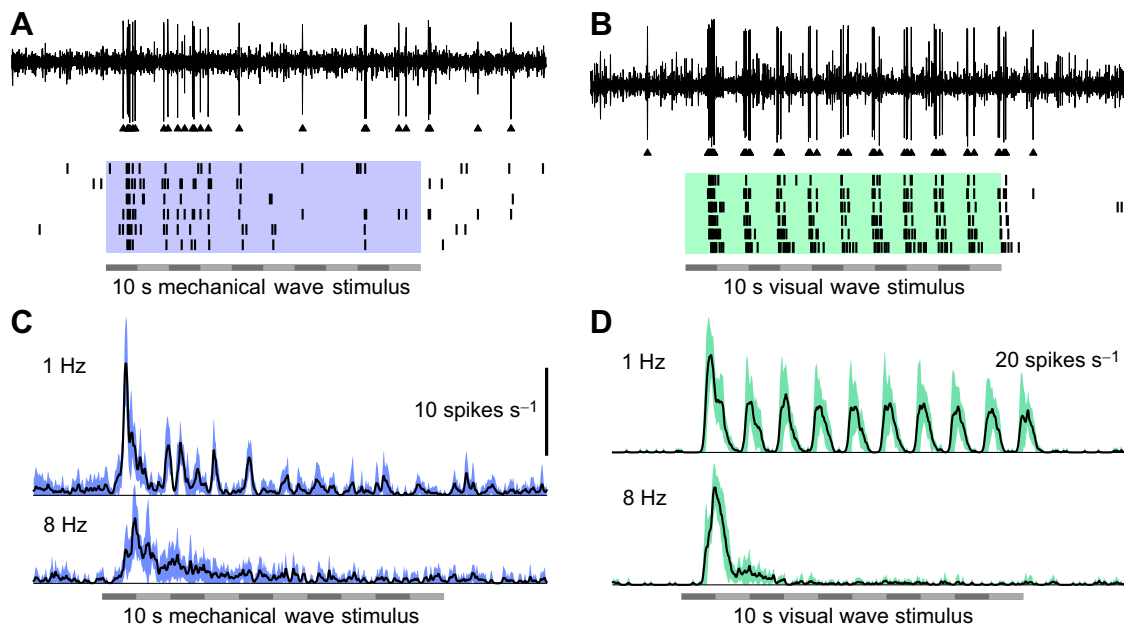


**Fig. 1. Medicinal leech *Hirudo verbana* S cell responses to mechanical and visual wave stimuli.** (A) Extracellular recording (top), detected spikes and raster plot (bottom) from an S cell responding to mechanically cued wave stimuli with a frequency of 1 Hz and an amplitude of 188  $\mu\text{m}$ . (B) Same for visually cued 1 Hz waves. (C) Average firing rate of the S cell in response to mechanically cued waves at 1 and 8 Hz (mean $\pm$ s.d.,  $N=8$  leeches). Wave amplitude was 188  $\mu\text{m}$  for the 1 Hz and 123  $\mu\text{m}$  for the 8 Hz waves. (D) Same for visually cued waves at 1 and 8 Hz ( $N=7$ ). Illuminance of all visual waves was 208 lux.

activity correlates with these behavioral findings, we exposed leeches to mechanically cued waves of 1–14 Hz and varying amplitudes, and to visually cued waves of 0.5–16 Hz.

For mechanical waves, the magnitude of the initial response (i.e. the number of spikes recorded during the initial phase, see Materials and methods) scaled approximately linearly with wave amplitude (Fig. 2A). A three-way ANOVA with frequency and amplitude as fixed factors and animal identity as a random factor demonstrated that wave frequency was a significant influence on the response ( $F_{9,304}=36.7$ ,  $P<10^{-15}$ ). A Tukey *post hoc* analysis ( $P<0.05$ ; lowercase letters in Fig. 2A) revealed that the response to high-frequency waves was strongest, in line with the behavioral results of Harley et al. (2011). Interestingly, responses were also elevated at around 3 Hz compared with both lower and higher frequencies. This had not previously been seen.

The sustained response to mechanical waves evinced very similar amplitude and frequency dependence as the initial response, even though firing rates were several fold lower overall (Fig. 2B; note that counts are over a much longer interval compared with Fig. 2A). In particular, frequency was again a significant factor ( $F_{9,304}=8.1$ ,  $P<10^{-10}$ ), and significant peaks in the response profile were seen at both the high end of the frequency range and around 3 Hz. However, the heights of these peaks were not distinguishable from each other.

For visual waves, the initial response was only mildly dependent on frequency (a two-way ANOVA with frequency and animal identity as factors yielded  $F_{5,240}=2.7$ ,  $P=0.02$ ; Fig. 2C). The sustained phase, however, was strongly dependent on frequency ( $F_{5,240}=49.5$ ,  $P<10^{-15}$ ; Fig. 2D). Furthermore, the frequency dependence was very different from the mechanical modality. Specifically, the response to low-frequency waves was significantly greater than to high-frequency waves (Tukey's test,  $P<10^{-6}$ ). This is largely in line with the behavioral findings of Harley et al. (2011), although the location of the peak was at 1 Hz rather than 2 Hz.

The frequency dependence of the sustained firing rates of the S cell in both visual and mechanical modalities approximately

matches the previously observed frequency dependence of unconstrained leeches finding wave sources. This suggests that the S cell may be involved in prey detection. However, successful prey capture also requires localization of the prey, i.e. determination of the direction of approaching waves. We therefore set out to determine whether the S cell may play a role in this process as well.

We presented leeches with mechanical waves directed towards the head or the tail of the animal or to either the left or right side, and measured the S cell responses. We tested 10 leeches with 1 and 8 Hz waves and counted spikes during the 10 s of each stimulus presentation. Although there was a slight trend for lower spike counts in response to waves directed towards the head, ANOVA revealed no significant differences as a function of wave direction at either frequency (Fig. 3A). This was also true when we only counted spikes in either the first 2 s of the stimulus or the last 5 s (data not shown).

We repeated this analysis with visually cued waves, and again found no effect of wave direction (Fig. 3B).

However, total spike counts are only part of the story. In all experiments thus far, we recorded S cell activity using a pair of electrodes around ganglion 10, which allowed us to not only confirm that the spikes that we recorded were truly S cell spikes, but also to determine the direction of their propagation (Fig. 3C; see Materials and methods). This revealed that in response to mechanical waves directed to the tail ('tail-on'), the vast majority of spikes propagated through segment 10 in a caudo-rostral direction, and hence originated posterior to ganglion 10 (Fig. 3D, top). A small secondary burst of rostro-caudally propagating spikes was observed shortly after the onset of the overall response; these spikes evidently originated anterior to ganglion 10. In contrast, mechanical waves directed to the head ('head-on'), first elicited a strong burst of spikes originating in the anterior, followed by more diffuse spiking from the posterior. In response to waves coming from the left or right side of the leech, the onset latencies of rostro-caudal and caudo-rostral spiking were equal to each other (Fig. S2A). For visual

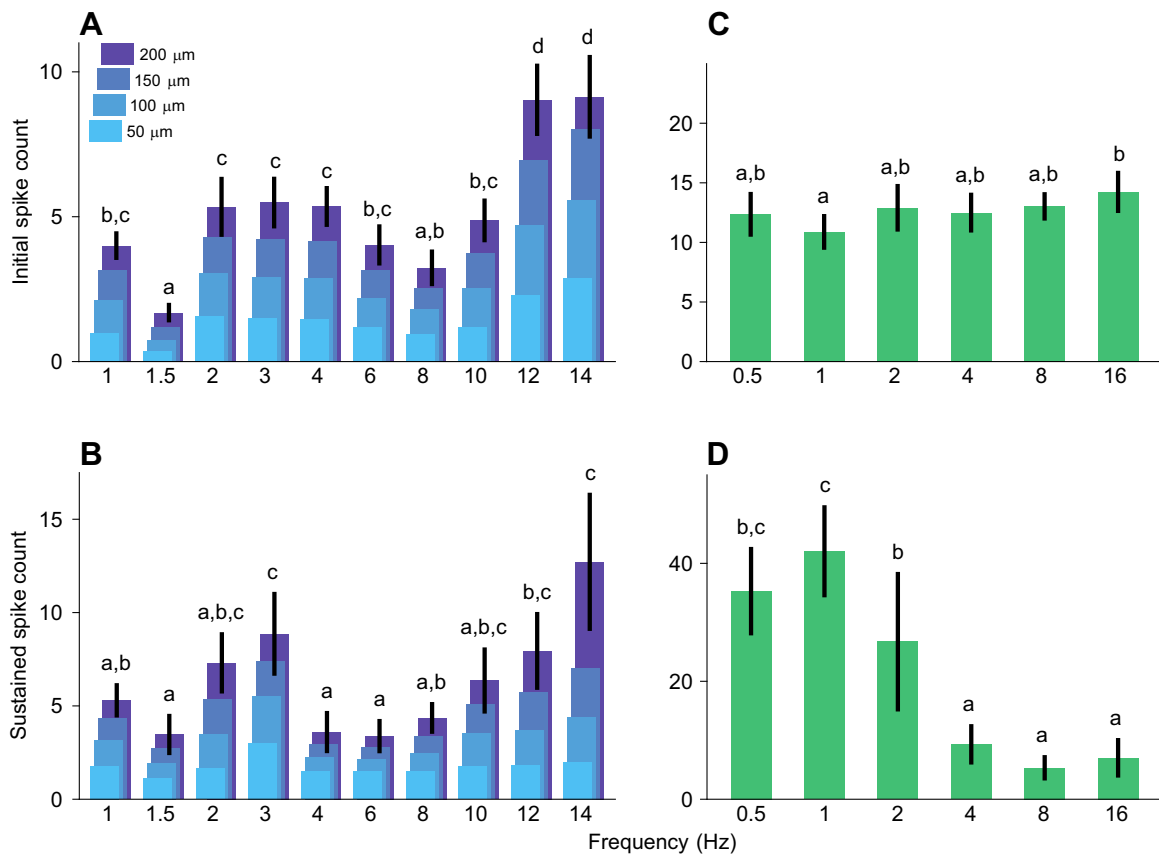


**Fig. 2. Frequency dependence of S cell responses.** (A) Spike counts in the initial phase of the response to mechanically cued waves with amplitudes of 50, 100, 150 and 200  $\mu\text{m}$  (see Data analysis in Materials and methods). Bars are averages from  $N=10$  leeches; error bars (s.e.m.) are shown only for 200  $\mu\text{m}$  waves. Lowercase letters indicate groupings from Tukey's test ( $P<0.05$ ) based on all amplitudes. (B) Spike counts in the sustained phase of the response to mechanically cued waves, as in A. (C) Spike counts in the initial response to visually cued waves;  $N=7$ . (D) Spike counts in the sustained phase of the response to visually cued waves, as in C.

waves (Fig. 3E; Fig. S2B), the situation was similar, although relatively fewer rostrocaudal spikes were observed in this modality.

Bagnoli et al. (1973) had shown that both mechanical and visual stimuli can enter the S cell system through nerve roots in individual mid-body segments, but they did not test how inputs from multiple segments interact, nor whether the head and tail brains play a role in this process. Therefore, we performed two series of ablation experiments to determine the roles of the various parts of the nervous system in transmitting visual responses.

In the first series, we recorded S-cell responses to full-body light flashes in leeches with intact nervous systems, prior to progressively ablating ganglia posterior to the recording site, to find out whether the caudorostral S cell spikes originated in the tail brain or in the posterior segmental ganglia. Unlike earlier results, which were all obtained with pairs of electrodes around ganglion 10, here we studied spike propagation around several ganglia (3, 10, 14 or 17). Around ganglia 10 and 14, the vast majority of spikes in response to trains of full-body flashes propagated in a caudorostral direction when the nervous system was intact (Fig. 4A). This was still true when the tail brain (TB) and one or two of the most posterior ganglia were ablated, indicating that the tail brain is not required for transmitting visual information to the S cell system. Sequential ablation of ganglia caused a gradual drop in caudorostral spikes. Only when almost all of the posterior ganglia were ablated, rostrocaudal spiking increased. This implies that the S cell system can be activated by visual information in anterior ganglia, but that

this generally does not happen when the nervous system is intact, probably because the S cell system is more readily activated in posterior ganglia. A similar pattern was seen around ganglion 3, although – surprisingly – the ablation of even a few posterior ganglia caused an increase in rostrocaudal spiking at this location. Lastly, around ganglion 17, rostrocaudal propagation dominated even when the nervous system was intact – perhaps because there are only four segments posterior to this recording site – and this dominance increased as posterior ganglia were ablated.

In the second series of ablation experiments, we studied local propagation of S cell spikes. We recorded around ganglion 10 as before, but we transected the nerve cord anterior to ganglion 7 and posterior to ganglion 13 to create a chain of seven ganglia still inside the leech. The nerve roots of ganglia 9–11 were cut as before, so that sensory input could only enter in segments 7–8 and 12–13. We recorded responses to sequences of three flashes with the same timing as above, but this time we used stimuli of several different light intensities. We found that caudorostral spikes dominated as they did in intact animals (Fig. 4B, left). Ablation of ganglia 12 and 13 caused a dramatic drop in caudorostral spikes ( $P=0.02$ , two-tailed  $t$ -test,  $N=3$ ) and an apparent increase in rostrocaudal spikes in each leech studied, although the  $t$ -test did not demonstrate significance. These results indicate that even locally, the posterior segments are a more potent initiator of S cell spikes. This experiment also demonstrates that the head brain is not required for the generation of rostrocaudal S cell spikes.

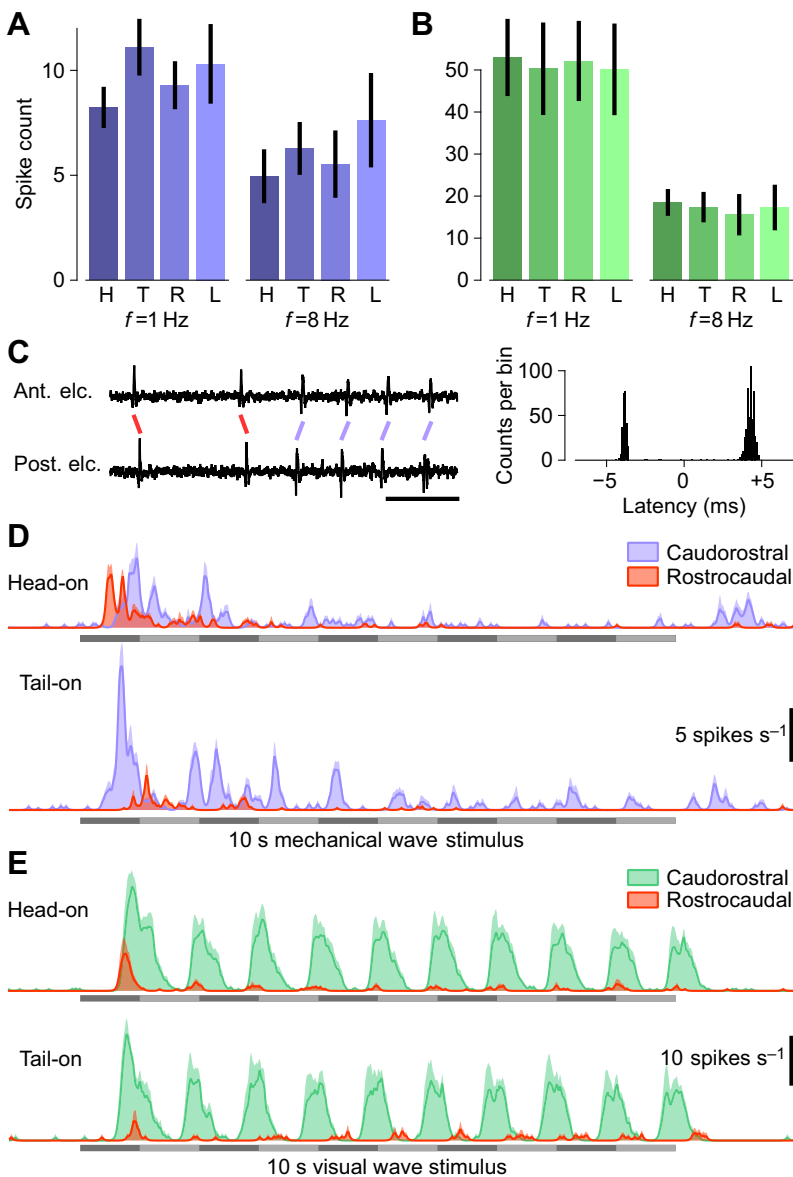


**Fig. 3. Dependence of S cell responses on wave direction.**

(A) S cell spike counts during 10 s of mechanical wave stimulation at 1 and 8 Hz for waves directed at the head (H), tail (T), right side (R) or left side (L) of the animal ( $N=8$  leeches).  $f$ , frequency. (B) Same for visually cued waves ( $N=7$  leeches). (C) Left: short segment of a recording using two electrodes, one anterior to ganglion 10 (Ant. elc., top trace), and one posterior to ganglion 10 (Post. elc., bottom trace), showing precisely timed paired spikes. Right: histogram of latencies within spike pairs showing two clearly distinct classes of pairs. Scale bar, 50 ms. (D) Rate of caudorostrally (tail-to-head; purple) and rostrocaudally (head-to-tail; red) propagating spikes in response to 1 Hz mechanical waves approaching the animal from the head (top) or tail (bottom). (E) Same for visually cued waves.

Ablating ganglia 7 and 8 instead of 12 and 13 had no significant effects on S cell spiking (Fig. 4C). This was probably because rostrocaudal spikes were already so rare in baseline that removing their source yielded no noticeable effect.

## DISCUSSION

Hungry leeches are highly motivated to localize the source of water disturbances. Behaviorally, they can use visual cues, mechanical cues, or a combination of the two to infer the presence of water waves and their direction of propagation (Dickinson and Lent, 1984; Carlton and McVean, 1993; Harley et al., 2011, 2013). Little has been known about processing of visual information in the leech, and less about processing of information relating to water movement. It was known, however, that one particular interneuron, the S cell, responds to both visual and mechanical stimuli (Bagnoli et al., 1973; Gardner-Medwin et al., 1973; Kretz et al., 1976; Sahley et al., 1994; Jellies, 2014). By presenting nearly intact leeches with natural water waves in complete darkness, we demonstrated that the S cell responds readily to purely mechanically cued water waves (Fig. 1A,C).

Likewise, by projecting patterns of light and darkness corresponding to propagating waves onto the dorsal surface of the leech, we demonstrated that the S cell responds to purely visually cued water waves (Fig. 1B,D). The responses to low-frequency waves consisted of clear bursts for each passing wave front, whereas at higher frequencies most of the response was in the form of only one burst at the onset of the stimulus. Any sustained response beyond this initial burst showed little phasic modulation. It is worth noting that in the response to low-frequency mechanically cued waves (Fig. 1C, top) a phase-locked pattern of bursts can also be discerned, but at twice the frequency of the wave. It is likely that both upward and downward phases of the wave cycle elicited small bursts of action potentials.

The S cell response to mechanically cued waves of different frequencies mostly agreed with the behaviorally measured rate of successful prey localization, except that we found a secondary peak of sensitivity around 3 Hz, which had not been seen in the behavioral study (Harley et al., 2011). It is possible, but unlikely, that this peak was missed in the earlier work study due to its coarser sampling of wave frequencies. In the case of visually cued waves,

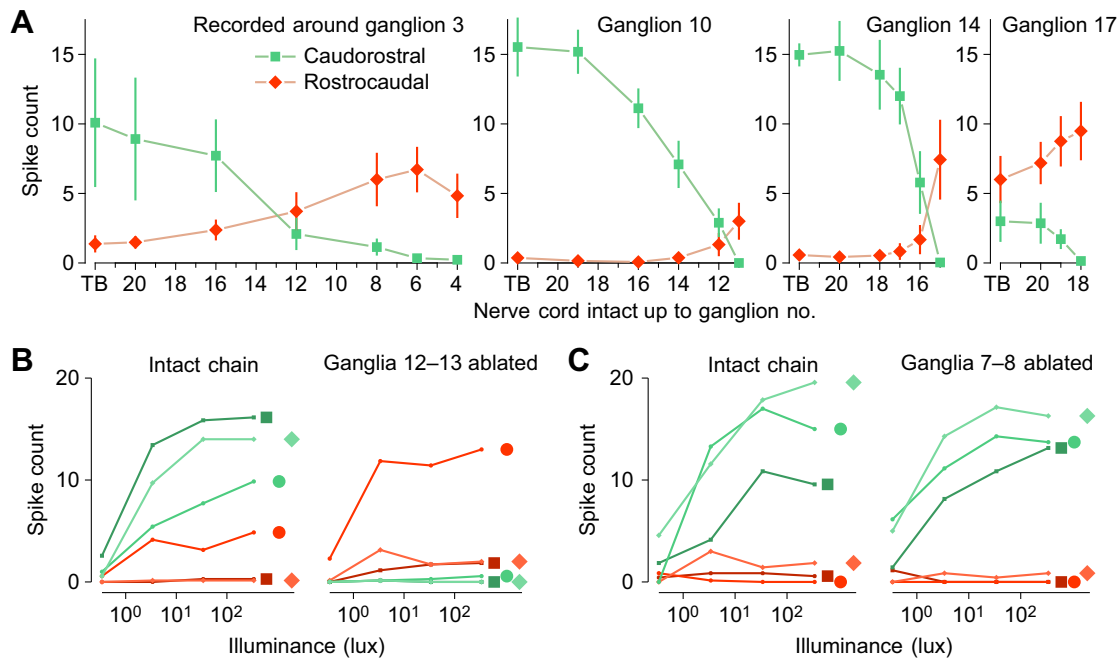


**Fig. 4. Effects of ablation of portions of the nervous system on S cell activity.** (A) Counts of caudorostral (green) and rostrocaudal (red) spikes in response to trains of three flashes (see Materials and methods) to the full dorsal surface of the leech at four different sites along the nerve cord in experiments where the posterior portion of the nervous system was progressively ablated. Values are means  $\pm$  s.e.m. of spike counts in the 2.5 s following stimulus onset from  $N=5$ , 4, 4 and 5 leeches at each of the four sites. TB, tail brain. Flash illuminance was 340 lux with 50% duty cycle. (B) Counts of caudorostral and rostrocaudal spikes around ganglion 10 in leeches in which the nerve cord was initially transected anterior to ganglion 7 and posterior to ganglion 13 ('intact chain'), in response to stimulus trains of varying illuminance, and again after ganglia 12 and 13 were ablated. Results from three leeches (identified by square, diamond and circle). (C) Same as B, except that ganglia 7 and 8 were ablated.

the initial S cell response was frequency independent but the sustained response mostly agreed with the behaviorally measured rate of successful prey localization (Fig. 2).

Overall, the response profile of the S cell resembled the behavioral response profile in many ways, but also differed from it in some important aspects. Based on the data presented here, it is impossible to conclude whether the S cell is directly involved in guiding the behavior: it remains possible that the S cell simply reflects the response profiles of the underlying sensory modalities. Further experiments recording directly from the sensory nerves will be required to test that idea; to our knowledge, no characterization of the sensory periphery of the leech in terms of its sensitivity to wave frequency presently exists in the literature.

We tested whether the S cell encodes information about the waves' propagation direction in its firing rate, but found that this was not the case at any of the wave frequencies tested (Fig. 3A,B). This result makes sense in view of the following two facts: first, there is only one S cell per ganglion, not a pair, and the S cell has a highly symmetric pattern of neurites (Peterson, 1984). This would make differentiation between leftward and rightward propagation difficult. Second, the electrical coupling between S cells in adjacent ganglia is extremely strong (Frank et al., 1975), so that an action potential initiated in any S cell typically propagates through the entire system. This would make differentiation between anterior and posterior wave propagation difficult. Nevertheless, we found that the S cell system does receive directional information about water waves: the direction of spike propagation within the S cell system depended on the direction of wave propagation (Fig. 3D,E). Although in all cases the majority of spikes propagated in the same direction as the waves, suggesting that the first spikes were initiated in the area where the wave first reaches the

animal. Whether the animal can make use of this information remains unknown. For this to occur, a downstream integration site would have to receive inputs from multiple sites along the S cell system and respond to those inputs in a differential fashion. We are not aware of any previously described neurons that could fill this role.

We found that neither the head nor the tail brain are required to generate an S cell response to visual stimuli. In fact, responses could be elicited in rather short chains of ganglia attached to the local sensory apparatus (Fig. 4B), suggesting that sensory information reaches the S cell system locally in each segment rather than through mediation by a remote integration site.

Nevertheless, not all segments are equal. As mentioned, the vast majority of S cell spikes recorded near the middle of the leech (in segments 10 and 14) traveled in a caudorostral direction (Figs 3D,E and 4A). This may be caused by the same mechanism that causes light flashes onto the tail of a leech to elicit more S cell spikes than light flashes onto the head (Jellies, 2014; Wagenaar and Stowasser, 2016). One possible explanation of these effects could be that posterior sensilla may be more sensitive to light and water motion than the anterior sensilla. Alternatively, the coupling between sensory receptors and S cells could be stronger in the posterior segments of the leech.

The S cell system has the fastest conduction velocity of all inter-ganglionic connections in the leech (Laverack, 1969; Gardner-Medwin et al., 1973; Frank et al., 1975). Accordingly, it was long believed that the S cell system played a central role in escape responses. However, Sahley et al. (1994) demonstrated that the S cell system is neither necessary nor sufficient for the initiation of whole-body shortening, a key escape response of the leech. (They also found that the S cell is activated during sensory-induced shortening and is required for normal plasticity of the shortening

response.) Our findings suggest that the S cell system may play a larger role in sensory integration in the context of predation. However, as it is unlikely that downstream target neurons can interpret the direction of spike propagation in the S cell system, the role of the S cells in predation appears limited to detection of a stimulus and arousal of the animal, and probably does not extend to subsequent localization of the source of that stimulus. Future experiments to directly test how the S cell responds to multimodal wave stimuli should be a high priority.

Leeches are not the only aquatic predators that integrate visual and mechanosensory cues to detect their prey. A notable vertebrate example is the mottled sculpin *Cottus bairdi*, of which lake and river populations weigh the two modalities differentially (Coombs and Grossman, 2006). Likewise, the hawkmoth *Manduca sexta* relies on the integration of these same two modalities to stabilize its flight (Roth et al., 2016). The leech, with its comparatively much smaller nervous system, cannot match these other animals in sophistication of behavior, but it presents a rare opportunity to study sensory integration in a simple and accessible nervous system.

#### Acknowledgements

We gratefully acknowledge help from Annette Stowasser in teaching dissection skills and useful discussions on optics and visual systems.

#### Competing interests

The authors declare no competing or financial interests.

#### Author contributions

Conceptualization: A.M., D.A.W.; Methodology: D.A.W.; Software: D.A.W.; Validation: D.A.W.; Formal analysis: A.M.L., A.M., D.A.W.; Investigation: A.M.L., A.M., D.A.W.; Data curation: D.A.W.; Writing - original draft: A.M.L., A.M., D.A.W.; Writing - review & editing: A.M.L., A.M., D.A.W.; Visualization: D.A.W.; Supervision: D.A.W.; Project administration: D.A.W.; Funding acquisition: D.A.W.

#### Funding

This work was supported by the Burroughs Wellcome Fund through a Career Award at the Scientific Interface and by the National Institute of Neurological Disorders and Stroke through R01 NS094403 (both to D.A.W.). Deposited in PMC for release after 12 months.

#### Supplementary information

Supplementary information available online at <http://jeb.biologists.org/lookup/doi/10.1242/jeb.171728.supplemental>

#### References

- Bagnoli, P., Brunelli, M. and Magni, F. (1973). Afferent connections to the fast conduction pathway in the central nervous system of the leech *Hirudo medicinalis*. *Arch. Ital. Biol.* **111**, 58-75.
- Bleckmann, H. and Barth, F. G. (1984). Sensory ecology of a semi-aquatic spider (*Dolomedes triton*) 2. The release of predatory behavior by water-surface waves. *Behav. Ecol. Sociobiol.* **14**, 303-312.
- Carlton, T. and McVean, A. (1993). A comparison of the performance of two sensory systems in host detection and location in the medicinal leech *Hirudo medicinalis*. *Comp Biochem. Physiol. Comp. Physiol.* **104**, 273-277.
- Coombs, S. and Grossman, G. D. (2006). Mechanosensory based orienting behaviors in fluvial and lacustrine populations of mottled sculpin (*Cottus bairdi*). *Mar. Freshwater Behav. Physiol.* **39**, 113-130.
- Dehnhardt, G., Mauck, B. and Bleckmann, H. (1998). Seal whiskers detect water movements. *Nature* **394**, 235-236.
- Dickinson, M. H. and Lent, C. M. (1984). Feeding behavior of the medicinal leech, *Hirudo medicinalis* L. *J. Comp. Physiol.* **154**, 449-455.
- Elepfandt, A. (1984). The role of ventral lateral line organs in water-wave localization in the clawed toad (*Xenopus laevis*). *J. Comp. Physiol.* **154**, 773-780.
- Frank, E., Jansen, J. K. and Rinvik, E. (1975). A multisomatic axon in the central nervous system of the leech. *J. Comp. Neurol.* **159**, 1-13.
- Gardner-Medwin, A. R., Jansen, J. K. S. and Tact, T. (1973). The 'giant' axon of the leech. *Acta Physiol. Scand.* **87**, 30A-31A.
- Hagiwara, S., Szabo, T. and Enger, P. S. (1965). Physiological properties of electroreceptors in the electric eel, *Electrophorus electricus*. *J. Neurophysiol.* **28**, 775.
- Harley, C. M., Cienfuegos, J. and Wagenaar, D. A. (2011). Developmentally regulated multisensory integration for prey localization in the medicinal leech. *J. Exp. Biol.* **214**, 3801-3807.
- Harley, C. M., Rossi, M., Cienfuegos, J. and Wagenaar, D. A. (2013). Discontinuous locomotion and prey sensing in the leech. *J. Exp. Biol.* **216**, 1890-1897.
- Horridge, G. A. and Boulton, P. S. (1967). Prey detection by Chaetognatha via a vibration sense. *Proc. Roy. Soc. Lond. B* **168**, 413ff.
- Jellies, J. (2014). Detection and selective avoidance of near ultraviolet radiation by an aquatic annelid: the medicinal leech. *J. Exp. Biol.* **217**, 974-985.
- Kretz, J. R., Stent, G. S. and Kristan, W. B. (1976). Photosensory input pathways in medicinal leech. *J. Comp. Physiol.* **106**, 1-37.
- Kristan, W. B., Stent, G. S. and Ort, C. A. (1974). Neuronal control of swimming in medicinal leech. 1. Dynamics of swimming rhythm. *J. Comp. Physiol.* **94**, 97-119.
- Lang, H. H. (1980). Surface-wave discrimination between prey and nonprey by the back swimmer *Notonecta glauca* L. (Hemiptera, Heteroptera). *Behav. Ecol. Sociobiol.* **6**, 233-246.
- Laverack, M. S. (1969). Mechanoreceptors, photoreceptors and rapid conduction pathways in the leech, *Hirudo medicinalis*. *J. Exp. Biol.* **50**, 129-140.
- Muller, K. J., Nicholls, J. G. and Stent, G. S. (eds.) (1981). *Neurobiology of the Leech*. Cold Spring Harbor, NY: Cold Spring Harbor Laboratory Press.
- Peterson, E. L. (1984). The fast conducting system of the leech - a network of 93 dye-coupled interneurons. *J. Comp. Physiol.* **154**, 781-788.
- Rizzoli, P. (2008). 12.802 Wave Motion in the Ocean and the Atmosphere. Spring 2008. Massachusetts Institute of Technology: MIT OpenCourseWare. <https://ocw.mit.edu/courses/earth-atmospheric-and-planetary-sciences/12-802-wave-motion-in-the-ocean-and-the-atmosphere-spring-2008/>.
- Röhlich, P. and Török, L. J. (1964). Elektronenmikroskopische Beobachtungen an den Sehzellen des Blutegels, *Hirudo medicinalis* L. *Zeitschrift für Zellforschung und Mikroskopische Anatomie* **63**, 618-635.
- Roth, E., Hall, R. W., Daniel, T. L. and Sponberg, S. (2016). Integration of parallel mechanosensory and visual pathways resolved through sensory conflict. *Proc. Natl. Acad. Sci. USA* **113**, 12832-12837.
- Russell, I. J. and Roberts, B. L. (1974). Active reduction of lateral-line sensitivity in swimming dogfish. *J. Comp. Physiol.* **94**, 7-15.
- Sahley, C. L., Modney, B. K., Boullis, N. M. and Muller, K. J. (1994). The S-cell: an interneuron essential for sensitization and full dishabituation of leech shortening. *J. Neurosci.* **14**, 6715-6721.
- Troyer, R. R. and Turner, A. M. (2015). Chemosensory perception of predators by larval amphibians depends on water quality. *PLoS ONE* **10**, e0131516.
- Wagenaar, D. A. (2015). A classic model animal in the 21st century: recent lessons from the leech nervous system. *J. Exp. Biol.* **218**, 3353-3359.
- Wagenaar, D. A. (2017). VScope - A software package for the acquisition and analysis of data from multiple cameras as well as electrophysiology. *J. Open Res. Software* **5**, 23.
- Wagenaar, D. A. and Stowasser, A. (2016). Visual responses of the S-cell system of the leech *Hirudo verbana* suggest complex integration mechanisms. In *Society for Neuroscience, 46th annual meeting, San Diego, CA*, abstract no 337.11.
- Wagenaar, D. A., Hamilton, M. S., Huang, T., Kristan, W. B., Jr. and French, K. A. (2010). A hormone-activated central pattern generator for courtship. *Curr. Biol.* **20**, 487-495.
- Wilkin, P. J. and Scofield, A. M. (1990). The use of a serological technique to examine host selection in a natural-population of the medicinal leech, *Hirudo medicinalis*. *Freshw. Biol.* **23**, 165-169.
- Wilson, M., Hanlon, R. T., Tyack, P. L. and Madsen, P. T. (2007). Intense ultrasonic clicks from echolocating toothed whales do not elicit anti-predator responses or debilitate the squid *Loligo pealeii*. *Biol. Lett.* **3**, 225-227.
- Young, S. R., Dedwylder, R. D. and Friesen, W. O. (1981). Responses of the medicinal leech to water-waves. *J. Comp. Physiol.* **144**, 111-116.
- Zimmer, C. (2001). Alternative life styles. *Nat. Hist.* **110**, 42-45.

# Responses to mechanically and visually cued water waves in the nervous system of the medicinal leech

## Supplemental material

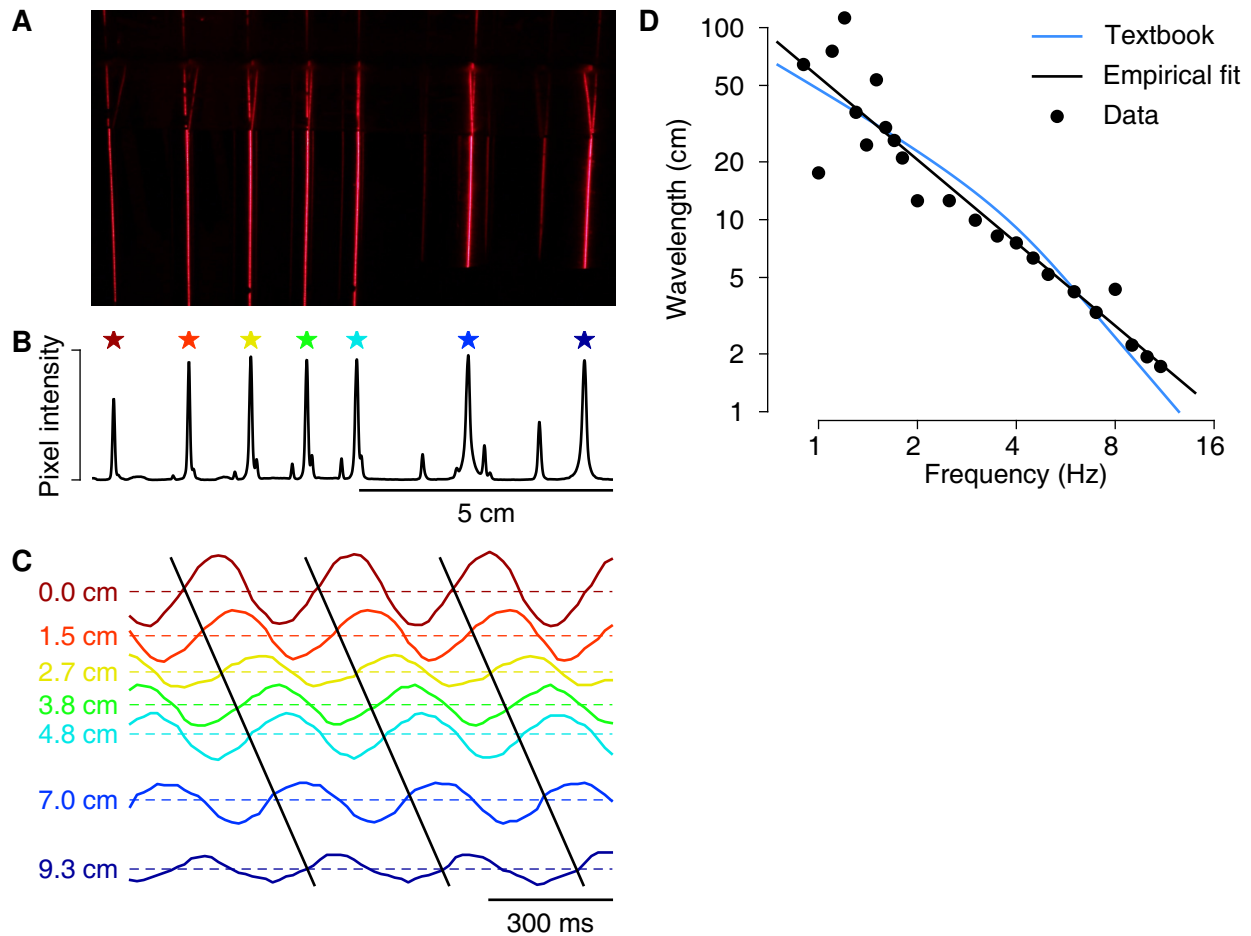


**Figure S1.** Determining the dispersion relation of physical waves. **A.** Photograph of the reflections of several shiny bars placed behind the aquarium. The bottom part of the reflection was used for measurements; the top part is a secondary reflection in the back wall of the aquarium. The bars are spaced irregularly to avoid aliasing of the measurements. **B.** Intensity profile across the image with peaks marked. **C.** Displacement of the reflections as a function of time during a 3-Hz wave. Colored traces correspond to points marked in (B). Vertical distance between traces is proportional to actual distance between bars. Displacement is exaggerated 50x. Black lines demonstrate linear propagation of the wave fronts.

**D. Results.** Data points are based on fitting a sine function

$$\Delta x(t) = A \sin(2\pi ft - \phi_x)$$

to the undulations of the reflections of a shiny metal bar placed behind the aquarium. In the equation,  $\Delta x$  is the observed displacement,  $f$  is the known frequency of the wave,  $t$  is time,  $x$  is the distance between the bar and the wave generator,  $A$  is an amplitude to be fitted, and  $\phi_x$  is a phase shift to be fitted. After determining  $\phi_x$  for a number of locations, we can calculate the wavelength  $\lambda$  of the wave by least-square fitting of  $\phi_x = \phi_0 + x/\lambda$ . Repeating this exercise for various frequencies  $f$  yielded the *black points*. The *black curve* is the best power law fit through the data:

$$1/\lambda = Af^B.$$

Least-square fitting of all our data (27 recordings at different frequencies) resulted in:

$$A = 0.0198 \pm 0.0014 \quad \text{and} \quad B = 1.414 \pm 0.033,$$

when frequencies were measured in hertz and wavelengths in centimeters. The *blue curve* is the textbook equation:

$$f = \sqrt{(g/2\pi\lambda) \tanh(2\pi h/\lambda)},$$

where  $h$  is the depth of the water (2.4 cm) and  $g$  is the gravity acceleration (9.81 m/s<sup>2</sup>). Note the logarithmic axes. Data at low frequencies are more scattered because of deviations from pure sinusoidal waves at the larger-than-typical wave amplitudes used for these experiments.

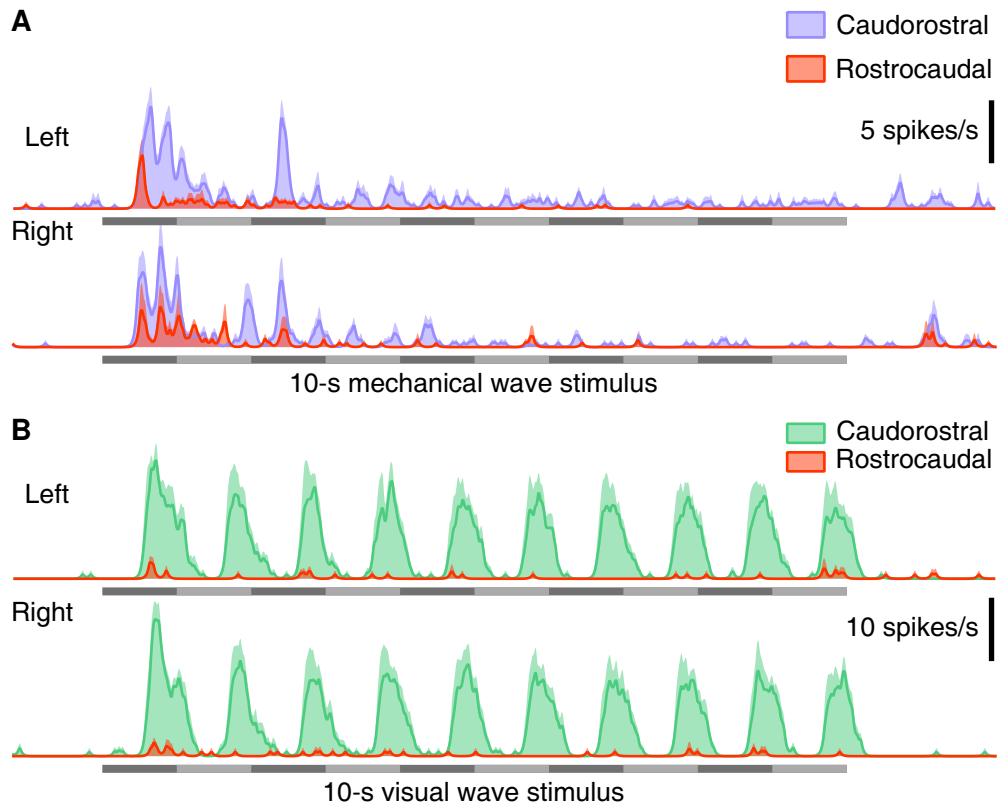


**Figure S2.** Dependence of S-cell responses on wave direction. **A.** Rate of caudorostrally (tail-to-head; purple) and rostrocaudally (head-to-tail) propagating spikes in response to 1-Hz mechanical waves approaching the animal from the left (top) or right (bottom). **B.** Same for visual waves. Compare to Figure 3D, E.